TECHNISCHE UNIVERSITÄT CHEMNITZ

Norman Lang Jens Saak Tatjana Stykel

Balanced truncation model reduction for linear time-varying systems

CSC/15-05

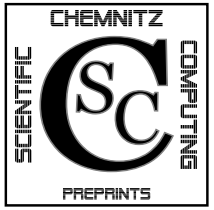

Chemnitz Scientific Computing Preprints

Chemnitz Scientific Computing Preprints – ISSN 1864-0087

Impressum:

Chemnitz Scientific Computing Preprints — ISSN 1864-0087
(1995–2005: Preprintreihe des Chemnitzer SFB393)

Herausgeber:
Professuren für
Numerische und Angewandte Mathematik
an der Fakultät für Mathematik
der Technischen Universität Chemnitz

Postanschrift:
TU Chemnitz, Fakultät für Mathematik
09107 Chemnitz
Sitz:
Reichenhainer Str. 41, 09126 Chemnitz

`http://www.tu-chemnitz.de/mathematik/csc/`

TECHNISCHE UNIVERSITÄT CHEMNITZ

Chemnitz Scientific Computing Preprints

Norman Lang Jens Saak Tatjana Stykel

Balanced truncation model reduction for linear time-varying systems

CSC/15-05

Abstract

A practical procedure based on implicit time integration methods applied to the differential Lyapunov equations arising in the square root balanced truncation method is presented. The application of high order time integrators results in indefinite right-hand sides of the algebraic Lyapunov equations that have to be solved within every time step. Therefore, classical methods exploiting the inherent low-rank structure often observed for practical applications end up in complex data and arithmetic. Avoiding the additional effort treating complex quantities, a symmetric indefinite factorization of both the right-hand side and the solution of the differential Lyapunov equations is applied.

CSC/15-05 ISSN 1864-0087 October 2015

Contents

1 Introduction 1

2 Balanced truncation for LTV systems 1

3 Solving differential Lyapunov equations 2
- 3.1 Backward Differentiation Formulas . . . 3
- 3.2 Rosenbrock methods . . . 4
  - 3.2.1 1-stage Rosenbrock method . . . 5
  - 3.2.2 2-stage Rosenbrock method . . . 6

4 Solving the reduced-order system 7

5 Numerical experiments 9
- 5.1 Example 1 . . . 9
- 5.2 Example 2 . . . 11
- 5.3 Example 3 . . . 11

6 Conclusion 14

Author's addresses:

Norman Lang
TU Chemnitz, Faculty of Mathematics
09107 Chemnitz, Germany
norman.lang@mathematik.tu-chemnitz.de

Jens Saak
Max Planck Institute for Dynamics of Complex Technical Systems
39106 Magdeburg, Germany
saak@mpi-magdeburg.mpg.de

Tatjana Stykel
Institut für Mathematik, Universität Augsburg
86159 Augsburg, Germany
stykel@math.uni-augsburg.de

[18] A. J. Laub, M. T. Heath, C. C. Paige, and R. C. Ward, *Computation of system balancing transformations and other application of simultaneous diagonalization algorithms*, IEEE Trans. Automat. Control, 32 (1987), pp. 115–122.

[19] J.-R. Li and J. White, *Low rank solution of Lyapunov equations*, SIAM J. Matrix Anal. Appl., 24 (2002), pp. 260–280.

[20] H. Mena, *Numerical Solution of Differential Riccati Equations Arising in Optimal Control Problems for Parabolic Partial Differential Equations*, Ph.D. thesis, Escuela Politecnica Nacional, 2007.

[21] T. Penzl, *Eigenvalue decay bounds for solutions of Lyapunov equations: the symmetric case*, Systems Control Lett., 40 (2000), pp. 139–144.

[22] T. Reis and T. Stykel, *Balanced truncation model reduction of second-order systems*, Math. Comput. Model. Dyn. Syst., 14 (2008), pp. 391–406.

[23] H. Sandberg, *Linear Time-Varying Systems: Modeling and Reduction*, Ph.D. thesis, Department of Automatic Control, Lund Institute of Technology, Lund, 2002.

[24] S. Shokoohi, L. Silverman, and P. Van Dooren, *Linear time-variable systems: balancing and model reduction*, IEEE Trans. Automat. Control, 28 (1983), pp. 810–822.

[25] M. S. Tombs and I. Postlethwaite, *Truncated balanced realization of a stable nonminimal state-space system*, Internat. J. Control, 46 (1987), pp. 1319–1330.

[26] E. I. Verriest and T. Kailath, *On generalized balanced realizations*, IEEE Trans. Automat. Control, 28 (1983), pp. 833–844.

[27] J. G. Verwer, E. J. Spee, J. G. Blom, and W. Hundsdorfer, *A second order Rosenbrock method applied to photochemical dispersion problems*, SIAM J. Sci. Comput., 20 (1999), pp. 1456–1480.

[5] P. Benner, R.-C. Li, and N. Truhar, *On the ADI method for Sylvester equations*, J. Comput. Appl. Math., 233 (2009), pp. 1035–1045.

[6] P. Benner and H. Mena, *Rosenbrock methods for solving Riccati differential equations*, IEEE Trans. Automat. Control, 58 (2013), pp. 2950–2957.

[7] P. Benner and J. Saak, *Linear-quadratic regulator design for optimal cooling of steel profiles*, Technical Report SFB393/05-05, TU Chemnitz, D-09107 Chemnitz, 2005. Available from http://www.tu-chemnitz.de/sfb393/sfb05pr.html.

[8] M. Bollhöfer and A. Eppler, *Low-rank Cholesky factor Krylov subspace methods for generalized projected Lyapunov equations*, in System Reduction for Nanoscale IC Design, P. Benner, ed., Mathematics in Industry, Springer-Verlag, 2016.

[9] C. Choi and A. J. Laub, *Efficient matrix-valued algorithms for solving stiff Riccati differential equations*, IEEE Trans. Automat. Control, 35 (1990), pp. 770–776.

[10] K. Dekker and J. G. Verwer, *Stability of Runge-Kutta methods for stiff nonlinear differential equations*, Elsevier, Amsterdam, North-Holland, 1984.

[11] L. Dieci, *Numerical integration of the differential Riccati equation and some related issues*, SIAM J. Numer. Anal., 29 (1992), pp. 781–815.

[12] V. Druskin and V. Simoncini, *Adaptive rational Krylov subspaces for large-scale dynamical systems*, Systems Control Lett., 60 (2011), pp. 546–560.

[13] S. K. Godunov, *Ordinary Differential Equations with Constant Coefficient*, vol. 169 of Translations of Mathematical Monographs, AMS, Providence, RI, 1997.

[14] E. Hairer and G. Wanner, *Solving Ordinary Differential Equations II - Stiff and Differential-Algebraic Problems*, vol. 14 of Springer Series in Computational Mathematics, Springer-Verlag, Berlin, Heidelberg, second ed., 2002.

[15] S. Hein, *MPC-LQG-Based Optimal Control of Parabolic PDEs*, Ph.D. thesis, TU Chemnitz, February 2009.

[16] T. Kailath, *Linear Systems*, Prentice-Hall, Englewood Cliffs, NJ, 1980.

[17] N. Lang, H. Mena, and J. Saak, *On the benefits of the LDL^T factorization for large-scale differential matrix equation solvers*, Linear Algebra Appl., 480 (2015), pp. 44–71.

1 Introduction

Consider a linear time-varying (LTV) control system

$$\begin{aligned} E(t)\dot{x}(t) &= A(t)x(t) + B(t)u(t), \quad x(0) = x_0, \\ y(t) &= C(t)x(t), \end{aligned} \tag{1}$$

where $E(t), A(t) \in \mathbb{R}^{n\times n}$, $B(t) \in \mathbb{R}^{n\times m}$ and $C(t) \in \mathbb{R}^{p\times n}$, $x_0 \in \mathbb{R}^n$ is the initial condition, $x(t) \in \mathbb{R}^n$ is the state vector, $u(t) \in \mathbb{R}^m$ is the input, and $y(t) \in \mathbb{R}^p$ is the output. The system matrices $E(t)$, $A(t)$, $B(t)$ and $C(t)$ are assumed to be continuous and bounded, and $E(t)$ is nonsingular for all $t \in [0, T]$. Furthermore, without loss of generality, we may assume that $x_0 = 0$. It is also possible to consider second-order systems that can be reformulated to systems of the form (1), see, e.g., [2, 22] and references therein.

In model order reduction, we aim to find a reduced-order model

$$\begin{aligned} \hat{E}(t)\dot{\hat{x}}(t) &= \hat{A}(t)\hat{x}(t) + \hat{B}(t)u(t), \quad \hat{x}(0) = \hat{x}_0, \\ \hat{y}(t) &= \hat{C}(t)\hat{x}(t), \end{aligned} \tag{2}$$

with $\hat{E}(t), \hat{A}(t) \in \mathbb{R}^{r\times r}$, $\hat{B}(t) \in \mathbb{R}^{r\times m}$ and $\hat{C}(t) \in \mathbb{R}^{p\times r}$ such that $r \ll n$ and the approximation error $\|\hat{y} - y\|$ is small in an appropriately chosen norm for all admissible inputs.

2 Balanced truncation for LTV systems

In this section, we briefly review a balanced truncation model order reduction method for LTV systems developed in [23, 24, 26]. This method relies on the *reachability* and *observability Gramians* $P(t)$ and $Q(t)$ defined for the LTV system (1) as the solutions of the differential Lyapunov equations (DLEs)

$$E(t)\dot{P}(t)E(t)^T = A(t)P(t)E(t)^T + E(t)P(t)A(t)^T + B(t)B(t)^T, \quad P(0) = 0, \tag{3}$$

$$-E(t)^T\dot{Q}(t)E(t) = A(t)^TQ(t)E(t) + E(t)^TQ(t)A(t) + C(t)^TC(t), \quad Q(T) = 0. \tag{4}$$

The initial and final conditions are directly given from the alternate integral representations

$$P(t) = \int_0^t \Phi(t,\tau)B(\tau)B(\tau)^T\Phi(t,\tau)^T d\tau,$$

$$Q(t) = \int_t^T \Phi(\tau,t)^TC(\tau)^TC(\tau)\Phi(\tau,t)d\tau$$

of the time-varying system Gramians, where $\Phi(t,\tau)$ is the transition matrix of the system, see, e.g., [16, Chapter 9.2]. Note that $P(t)$ and $Q(t)$ are both symmetric and positive semidefinite for all $t \in [0,T]$. Then the product $P(t)E(t)^TQ(t)E(t)$ has real nonnegative eigenvalues $\lambda_i\big(P(t)E(t)^TQ(t)E(t)\big)$. The *Hankel singular values* (HSV) of system (1) are defined as

$$\sigma_i(t) = \sqrt{\lambda_i\big(P(t)E(t)^TQ(t)E(t)\big)}, \qquad i = 1,\ldots,n\,.$$

We assume that the Hankel singular values are ordered decreasingly, i.e.,

$$\sigma_1(t) \geq \cdots \geq \sigma_n(t), \quad t \in [0,T].$$

The LTV system (1) is called *balanced* if $P(t) = Q(t) = \operatorname{diag}(\sigma_1(t),\ldots,\sigma_n(t))$ for all $t \in [0,T]$. Under certain conditions on system (1), see [24, 26], one can find nonsingular system transformation matrices $W_b(t)$ and $Z_b(t)$ such that $Z_b(t)$ is continuously differentiable and the transformed system

$$\begin{aligned} W_b^T(t)E(t)Z_b(t)\dot{x}_b(t) &= W_b^T(t)\big(A(t)Z_b(t) - E(t)\dot{Z}_b(t)\big)x_b(t) + W_b^T(t)B(t)u(t),\\ y(t) &= C(t)Z_b(t)x_b(t) \end{aligned} \tag{5}$$

is balanced. Then a reduced-order model (2) can be determined by truncating the states of (5) corresponding to the small Hankel singular values. In practice, we do not need to construct the balancing transformations $W_b(t)$ and $Z_b(t)$ explicitly. Instead, the reduced-order model (2) can be computed by Algorithm 1, which is a generalization of a square root balanced truncation method developed in [18, 25] for linear time-invariant systems.

3 Solving differential Lyapunov equations

In this section, we discuss the numerical solution of the DLE (3). The dual DLE (4) has to be solved backward in time. Substituting t with $T-t$ and introducing the matrices $E_T(t) = E(T-t)$, $A_T(t) = A(T-t)$, $B_T(t) = B(T-t)$, $C_T(t) = C(T-t)$ and $Q_T(t) = Q(T-t)$, we obtain the DLE

$$\begin{aligned} E_T^T(t)\dot{Q}_T(t)E_T(t) &= A_T^T(t)Q_T(t)E_T(t) + E_T^T(t)Q_T(t)A_T(t) + C_T^T(t)C_T(t),\\ Q_T(0) &= 0. \end{aligned} \tag{7}$$

This initial value problem can then be solved analogously to (3). Note that the DLE can be considered as a special case of the differential Riccati equation (DRE). Therefore, any integration method developed for the DREs [6, 9, 11, 20] can also be employed for the DLEs. Here, we consider the backward differentiation formulas (BDF) and the Rosenbrock methods only.

solved inside the time integrators, complex data and arithmetic can be avoided. The numerical results show that the proposed integration methods yield satisfactory approximation with respect to the relative errors in the system outputs of the full and the reduced-order models. An interesting issue that needs to be discussed in the future is the initial and final condition of the reachability and observability Gramians, respectively. These conditions force the reduced state $\hat{x}(t)$ to be zero at the temporal boundaries, i.e., $\hat{x}(0) = \hat{x}(T) = 0$, even if the full order state fulfills $x(0) \neq 0$ and $x(T) \neq 0$. For practical computations it seems to be necessary to embed the time horizon $[0,T]$ of interest in a sufficiently large interval $[0-\delta, T+\delta]$ with $\delta > 0$.

Acknowledgements

The first two authors were funded by the DFG project "*Collaborative Research Center/ Transregio 96 Thermo-Energetic Design of Machine Tools*". The third author was supported by the DFG project "*Model reduction for elastic multibody systems with moving interactions*". Furthermore, the authors like to thank Maximilian Huber for providing the heated beam example.

References

[1] P. Benner, S. Görner, and J. Saak, *Numerical solution of optimal control problems for parabolic systems*, in Parallel Algorithms and Cluster Computing. Implementations, Algorithms, and Applications, K. H. Hoffmann and A. Meyer, eds., vol. 52 of Lect. Notes Comput. Sci. Eng., Springer-Verlag, Berlin/Heidelberg, Germany, 2006, pp. 151–169.

[2] P. Benner, P. Kürschner, and J. Saak, *Improved second-order balanced truncation for symmetric systems*, in Proceedings of the 7th Vienna International Conference on Mathematical Modelling (MATHMOD 2012), I. Troch and F. Breitenecker, eds., vol. 7 of Mathematical Modelling, IFAC-PapersOnLine, 2012, pp. 758–762.

[3] P. Benner, P. Kürschner, and P. Saak, *Efficient handling of complex shift parameters in the low-rank Cholesky factor ADI method*, Numer. Algorithms, 62 (2013), pp. 225–251.

[4] ——, *A reformulated low-rank ADI iteration with explicit residual factors*, Proc. Appl. Math. Mech., 13 (2013), pp. 585–586.

trajectory x_{ref} is applied. The resulting linear time-varying model reads

$$\begin{aligned} E\dot{x}(t) &= A(t)\,(x(t) - x_{ref}(t)) + Bu(t) + f(t, x_{ref}(t)) \\ &= A(t)x(t) + Bu(t) + \tilde{f}(t, x_{ref}(t)), \\ y &= Cx(t) \end{aligned} \tag{22}$$

with $E = I_n$ and a time dependency given solely in $A(t)$. For details on the linearization and discretization the authors refer to [15] and the references given therein. We consider a single-input-single-output system of dimension $n = 2\,500$. The matrix $B \in \mathbb{R}^n$ is constructed in a way such that the input acts on a grid region of 1% of the grid nodes around the middle of the spatial domain $(0, 1)$. That is, $B_i = 1$ for $i = \mathsf{floor}(\frac{n}{2}) \pm \mathsf{floor}(0.01n)$ and zero, otherwise. Here, floor denotes the MATLAB® built-in function that rounds the argument to the nearest integer value towards zero. The matrix $C \in \mathbb{R}^{1\times n}$ observes the grid point 5 spatial steps to the right of the middle point, i.e., $C_i = 1$ for $i = \mathsf{floor}(\frac{n}{2}) + 5$ and zero otherwise.

Note that the inhomogeneity $\tilde{f}(t, x_{ref})$ in (22) does not affect the model reduction procedure. Following the procedure in [1] for tracking control based on a common trick to handle inhomogeneities presented in e.g., [13], system (22) can be reformulated into a state-space system (1) while the system matrices do not change.

The model is simulated on the time horizon $[0, 3]s$ with time step size $\tau = (2e\text{-}2)s$. The input is chosen to be $u(t) = 2(\sin(2\pi t) + 1)$, where $u(t) \in [0, 4]$ for $t \in [0, T]$. The truncation tolerance for the HSVs was $1e$-7. Analogously to the previous examples, Figure 3 depicts the dimensions of the reduced order models with respect to the DLE solution methods (a), the Hankel singular values σ_1, σ_3, and σ_6 (b), the HSV decay over time (c), the output trajectories of the full and the reduced-order models (d), as well as the corresponding relative errors (e). For some reason using the first-order Rosenbrock method results in an erroneous behavior of the Hankel singular values. This might be the explanation for the slightly worse fit of the corresponding reduced-order output and needs to be investigated in the future.

6 Conclusion

In the paper, we have presented the BDF and Rosenbrock time integration methods for the solution of the differential Lyapunov equations arising in the balanced truncation square root method for linear time-varying dynamical systems. Using a low-rank symmetric indefinite factorization for the solution and the indefinite right-hand sides of the algebraic Lyapunov equations, that have to be

Algorithm 1 Balanced truncation for LTV systems.

Require: $\big(E(t), A(t), B(t), C(t)\big)$

Ensure: a reduced-order system $\big(\hat{E}(t), \hat{A}(t), \hat{B}(t), \hat{C}(t)\big)$

1: Compute the Cholesky factors $R(t)$ and $L(t)$ of the reachability and observability Gramians $P(t) = R(t)R^T(t)$ and $Q(t) = L(t)L^T(t)$ satisfying the DLEs (3) and (4), respectively.

2: Compute the singular value decomposition

$$R^T(t)E^T(t)L(t) = [\,U_1(t),\, U_2(t)\,] \begin{bmatrix} \Sigma_1(t) & \\ & \Sigma_2(t) \end{bmatrix} [\,V_1(t),\, V_2(t)\,]^T,$$

where the matrices $[\,U_1(t), U_2(t)\,]$ and $[\,V_1(t), V_2(t)\,]$ have orthonormal columns, $\Sigma_1(t) = \mathrm{diag}(\sigma_1(t), \ldots, \sigma_r(t))$ and $\Sigma_2(t) = \mathrm{diag}(\sigma_{r+1}(t), \ldots, \sigma_n(t))$.

3: Compute the reduced-order system (2) with

$$\begin{aligned} \hat{E}(t) &= W^T(t)E(t)Z(t), & \hat{A}(t) &= W^T(t)\big(AZ(t) - E(t)\dot{Z}(t)\big), \\ \hat{B}(t) &= W^T(t)B(t), & \hat{C}(t) &= C(t)Z(t), \end{aligned} \tag{6}$$

where $W(t) = L(t)V_1(t)\Sigma_1^{-1/2}(t)$ and $Z(t) = R(t)U_1(t)\Sigma_1^{-1/2}(t)$.

In the remainder, as a representative of the DLEs (3) and (7), we consider the DLE

$$E(t)\dot{X}(t)E^T(t) = F(t, X(t)), \quad X(0) = 0, \tag{8}$$

where

$$F(t, X(t)) = A(t)X(t)E^T(t) + E(t)X(t)A^T(t) + N(t)N^T(t)$$

with $E(t), A(t)$ as before and $N(t) \in \mathbb{R}^{n\times\tilde{n}(t)}$, $\tilde{n}(t) \ll n$ for all $t \in [0, T]$. Let τ_k be the time step size and let $t_0 = 0 < t_1 < \ldots < t_q = T$ with $q \in \mathbb{N}$ be a discretization of the time interval $[0, T]$ with $t_{k+1} = t_k + \tau_k$, $k = 0, \ldots, q-1$.

3.1 Backward Differentiation Formulas

The s-step BDF method applied to equation (8) has the form

$$E(t_k)\big(\sum_{j=0}^{s} \alpha_j X_{k-j}\big)E^T(t_k) = \tau_k \beta F(t_k, X_k),$$

where X_k is an approximation to $X(t_k)$, and the coefficients α_j and β are given in Table 1. These coefficients are chosen such that the s-step BDF method has the maximum possible order s. Setting $E_k = E(t_k)$, $A_k = A(t_k)$ and $N_k = N(t_k)$

and assuming that $X_0, \ldots, X_{k-1}$ are already known, the matrix X_k can then be determined from the algebraic Lyapunov equation (ALE)

$$\tilde{A}_k X_k E_k^T + E_k X_k \tilde{A}_k^T = -\tau_k \beta N_k N_k^T + E_k \Big(\sum_{j=1}^{s} \alpha_j X_{k-j}\Big) E_k^T \tag{9}$$

with $\tilde{A}_k = \tau_k \beta A_k - \frac{\alpha_0}{2} E_k$. If the pencil $\lambda E_k - A_k$ is stable, i.e., all its eigenvalues have negative real part, then $\lambda E_k - \tilde{A}_k$ is stable too. In this case, the ALE (9) is uniquely solvable. For large-scale problems, it is recommended to never compute the full solutions X_k, $k = 1, \ldots, q$. Since in practice the solutions X_k have often numerically low ranks, low-rank solution methods [3, 4, 19, 21] should be applied to the ALE (9). Note that for $s \geq 2$ some of the coefficients α_j, $j = 1, \ldots, s$, are positive, and hence the right-hand side (rhs) of (9) may become indefinite. If the matrices X_j, $j = 0, \ldots, k-1$, admit a so-called low-rank *symmetric indefinite factorization* $X_j \approx L_j D_j L_j^T$ with $L_j \in \mathbb{R}^{n \times \ell_j}$, symmetric $D_j \in \mathbb{R}^{\ell_j \times \ell_j}$ and $\ell_j \ll n$, then the rhs of the ALE (9) can be approximated by

$$-\tau_k \beta N_k N_k^T + E_k \Big(\sum_{j=1}^{s} \alpha_j X_{k-j}\Big) E_k^T \approx -G_k S_k G_k^T,$$

where the factors G_k and S_k are given by

$$G_k = \begin{bmatrix} N_k, & E_k L_{k-1}, & \ldots, & E_k L_{k-s} \end{bmatrix},$$
$$S_k = \begin{bmatrix} \tau_k \beta I_{\tilde{n}_k} & & & \\ & -\alpha_1 D_{k-1} & & \\ & & \ddots & \\ & & & -\alpha_s D_{k-s} \end{bmatrix}. \tag{10}$$

In this case, an approximate solution of the ALE (9) can be determined in the factorized form $X_k \approx L_k D_k L_k^T$ using the LDL^T-type ADI or Krylov method presented in [5, 17], respectively. Note that the application of the symmetric indefinite factorization based solvers is recommended in order to avoid complex data and arithmetic which is introduced by classical low-rank factorization of the indefinite rhs. Since the rhs low-rank factors will increase within each time integration step, it is desirable to perform a column compression as proposed in [8] in order to reduce the number of columns of these factors and, as a consequence, to reduce the computational complexity of solving the ALE (9).

3.2 Rosenbrock methods

Following the descriptions for DREs in [6, 17, 20], a general s-stage Rosenbrock method, as defined in [10, Chapter 9], applied to the DLE (8) with a constant

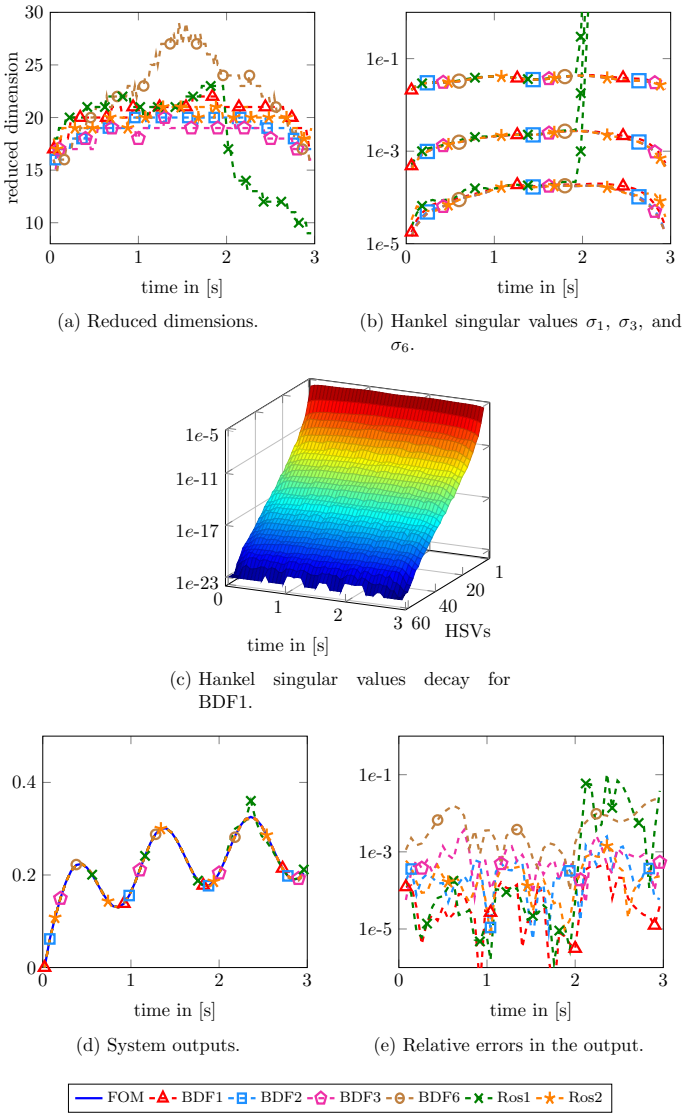

(a) Reduced dimensions.

(b) Hankel singular values σ_1, σ_3, and σ_6.

(c) Hankel singular values decay for BDF1.

(d) System outputs.

(e) Relative errors in the output.

Figure 3: Burgers equation: (a) dimensions of the reduced state at different times, (b) the Hankel singular values σ_1, σ_3, and σ_6 for the BDF methods of order 1, 2, 3, and 6 and the Rosenbrock schemes of order 1 and 2, (c) Hankel singular values for the BDF method of order 1, (d) the outputs of the full and the reduced-order models, and (e) relative errors in the output.

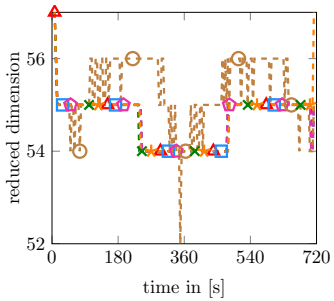

(a) Reduced dimensions.

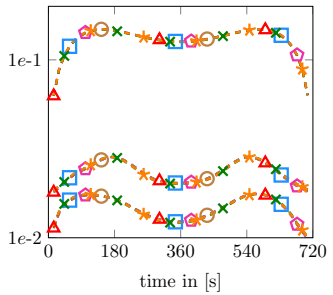

(b) Hankel singular values σ_1, σ_3, and σ_6.

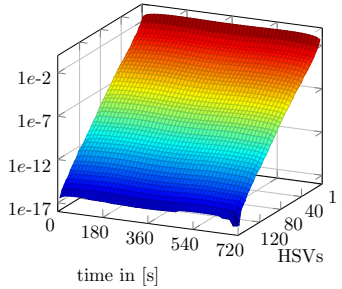

(c) Hankel singular values decay for BDF1.

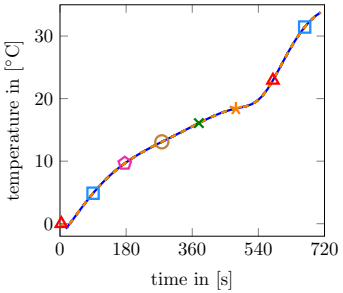

(d) System outputs.

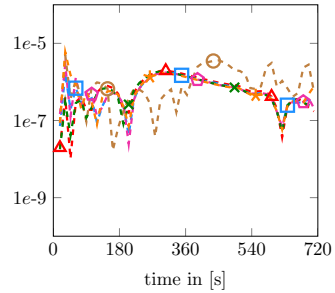

(e) Relative errors in the output.

Figure 2: Steel profile: (a) dimensions of the reduced state at different times, (b) the Hankel singular values σ_1, σ_3, and σ_6 for the BDF methods of order 1, 2, 3, and 6 and the Rosenbrock schemes of order 1 and 2, (c) Hankel singular values for the BDF method of order 1, (d) the outputs of the full and the reduced-order models, and (e) relative errors in the output.

s	β	α_0	α_1	α_2	α_3	α_4	α_5	α_6
1	1	1	-1					
2	2	3	-4	1				
3	6	11	-18	9	-2			
4	12	25	-48	36	-16	3		
5	60	137	-300	300	-200	75	-12	
6	60	147	-360	450	-400	225	-72	10

Table 1: Coefficients of the s-step BDF method.

mass matrix $E(t) \equiv E$, reads

$$\begin{aligned} X_{k+1} &= X_k + \sum_{i=1}^{s} b_i K_i, \\ A_{ki} K_i E^T + E K_i A_{ki}^T &= -F\big(t_k + \alpha_i \tau_k, X_k + \sum_{j=1}^{i-1} a_{ij} K_j\big) - \sum_{j=1}^{i-1} \frac{c_{ij}}{\tau_k} E K_j E^T. \end{aligned} \tag{11}$$

In the literature many authors, see e.g., [14, Section IV.7], start their explanations for autonomous ODE systems. Then a general Rosenbrock scheme for non-autonomous ODEs is based on an autonomization and thus yields

$$\begin{aligned} X_{k+1} &= X_k + \sum_{i=1}^{s} b_i K_i, \\ A_{ki} K_i E^T + E K_i A_{ki}^T &= -F\big(t_k + \alpha_i \tau_k, X_k + \sum_{j=1}^{i-1} a_{ij} K_j\big) - \sum_{j=1}^{i-1} \frac{c_{ij}}{\tau_k} E K_j E^T - \gamma_i \tau_k F_{t_k}. \end{aligned}$$

In both cases $A_{ki} = A(t_k) - \frac{1}{2\gamma_{ii}\tau_k} E$ and b_i, α_i, a_{ij}, c_{ij}, γ_i, and γ_{ii} are the method coefficients. In the latter scheme, defined for non-autonomous ODEs being autonomized, F_{t_k} denotes the time derivative $\frac{\partial F}{\partial t}(t_k, X(t_k))$ of F at $(t_k, X(t_k))$. This term may be disadvantageous for the stability of the method, see [10, Chapter 9.5] for details. Therefore, in the remainder, we neglect the time derivative F_{t_k} and restrict our considerations to scheme (11) defined for non-autonomous ODEs.

3.2.1 1-stage Rosenbrock method

The 1-stage Rosenbrock scheme

$$\begin{aligned} X_{k+1} &= X_k + K_1, \\ A_{k1} K_1 E^T + E K_1 A_{k1}^T &= -F\big(t_k, X_k\big) \end{aligned} \tag{12}$$

with $b_1 = \gamma_{11} = 1$ and $\alpha_1 = 0$ represents the linear implicit Euler scheme of first order. Substituting $K_1 = X_{k+1} - X_k$ into the ALE (12), we obtain the ALE

$$A_{k1}X_{k+1}E^T + EX_{k+1}A_{ki}^T = -N_kN_k^T - \frac{1}{\tau_k}EX_kE^T. \tag{13}$$

Note that starting with $X_0 = 0$, the solution X_{k+1}, $k = 0, \ldots, q-1$, of the ALE (13) is symmetric, positive semidefinite provided the pencil $\lambda E - A_{k1}$ is stable. Assuming the low-rank factorization $X_k \approx Y_kY_k^T$, the rhs of the ALE (13) can be written as

$$-N_kN_k^T - \frac{1}{\tau_k}EX_kE^T \approx -\left[N_k, \quad \frac{1}{\sqrt{\tau_k}}EY_k\right]\left[N_k, \quad \frac{1}{\sqrt{\tau_k}}EY_k\right]^T.$$

Therefore, the classical low-rank ADI or (rational) Krylov subspace method [3, 12] can be used for computing a low-rank solution of the ALE (13).

3.2.2 2-stage Rosenbrock method

Based on the formulations for the DRE in [6, 20], the 2-stage Rosenbrock scheme from [27] applied to the DLE (8) is given by

$$\begin{aligned} X_{k+1} &= X_k + \frac{3}{2}K_1 + \frac{1}{2}K_2, \\ \tilde{A}_kK_1E^T + EK_1\tilde{A}_k^T &= -F(t_k, X_k) && (14) \\ \tilde{A}_kK_2E^T + EK_2\tilde{A}_k^T &= -F(t_k + \tau_k, X_k + K_1) + \frac{2}{\tau_k}EK_1E^T && (15) \end{aligned}$$

with $\tilde{A}_k = \gamma A(t_k) - \frac{1}{2\tau_k}E$. Now, we assume that the solutions at the previous time steps are given by $X_k \approx L_kD_kL_k^T$. Therefore, for the rhs of the first stage equation (14), we obtain the low-rank symmetric indefinite factorization

$$F(t_k, X_k) = N_kN_k^T + A_kX_kE^T + EX_kA_k^T \approx G_{k1}S_{k1}G_{k1}^T$$

with the factors

$$G_{k1} = \begin{bmatrix} N_k, & A_kL_k, & EL_k \end{bmatrix}, \qquad S_{k1} = \begin{bmatrix} I_{\bar{n}_k} & & \\ & & D_k \\ & D_k & \end{bmatrix}.$$

Then the solution K_1 of (14) can be determined in a factorized form $K_1 \approx R_1M_1R_1^T$ with $R_1 \in \mathbb{R}^{n\times r_1}$ and $M_1 \in \mathbb{R}^{r_1\times r_1}$. In this case, the rhs of the second stage equation (15) can be written as

$$\begin{aligned} F(t_k + \tau_k, X_k + K_1) - \frac{2}{\tau_k}EK_1E^T &= N_{k+1}N_{k+1}^T + A_{k+1}X_kE^T + EX_kA_{k+1}^T \\ &\quad + A_{k+1}K_1E^T + EK_1A_{k+1}^T - \frac{2}{\tau_k}EK_1E^T \\ &\approx G_{k2}S_{k2}G_{k2}^T \end{aligned}$$

time integrators show basically the same results with slight advantages for the BDF methods in particular in the time range of $t \in [20, 80]$. The behavior of the Hankel singular values appears to be identical for all integration methods, see Figure 1(b). This is, of course, expected, as long as the time integrators find the "correct" solution to the DLEs (3) and (4).

5.2 Example 2

The second example describes a heat transfer model originating from an optimal cooling problem for the steel profile given in [7]. In order to obtain an LTV model, we have introduced an artificial time variability to the heat conduction coefficient entering the system matrix A. As a result, we have the system (1) with constant matrices E, B, C and a time-varying system matrix $A(t)$. This system has dimension $n = 1357$, $m = 7$ inputs and $p = 6$ outputs. The solution is computed on the time interval $[0, 720]s$ with a time integration step size of $\tau = 3.6s$ and an input $u(t) = 50\ ^\circ C$ describing the heating of the steel profile. The Hankel singular values were truncated at a tolerance of $1e$-5. As for the first example, Figure 2 shows the reduced orders obtained by the different DLE solvers (a), the Hankel singular values σ_1, σ_3, and σ_6 (b), and the Hankel singular values decay (c). Further, Figures 2(d) and 2(e) depict the output trajectories of the full and the reduced-order models, as well as the associated relative errors, respectively. In terms of their quality, these results are similar to those in the example above. One can see that the Hankel singular values are again almost invariant with respect to the integration method used to compute the time-varying system Gramians.

5.3 Example 3

In the third example, we consider the Burgers equation

$$\begin{aligned} &\dot{x}(t,z) = \nu\frac{\partial^2}{\partial z^2}x(t,z) - x(t,z)\frac{\partial}{\partial z}x(t,z) + u(t,z), && (t,z) \in (0,T)\times(0,1), \\ &x(t,0) = 0, \quad x(t,1) = 0, && t \in (0,T), \\ &x(0,z) = x_0(z), && z \in (0,1). \end{aligned} \tag{21}$$

A spatial discretization using finite differences yields a non-linear model equation. In order to obtain a linear model a linearization around a pre-computed reference

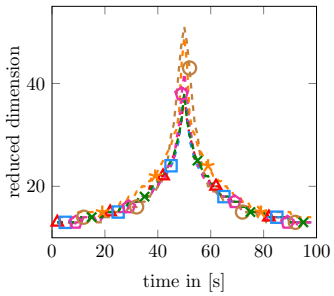

(a) Reduced dimensions.

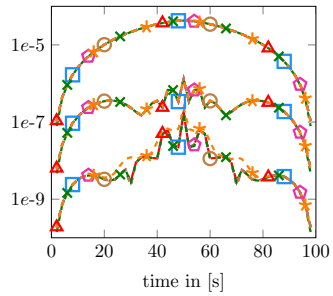

(b) Hankel singular values σ_1, σ_3, and σ_6.

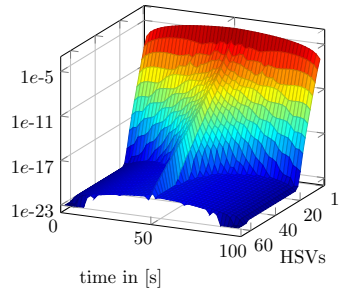

(c) Hankel singular values decay for BDF1.

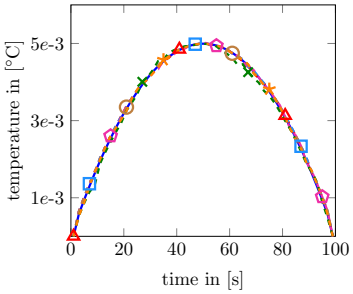

(d) System outputs.

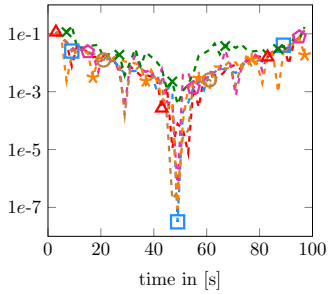

(e) Relative errors in the output.

Figure 1: Heated beam: (a) dimensions of the reduced state at different times, (b) the Hankel singular values σ_1, σ_3, and σ_6 for the BDF methods of order 1, 2, 3, and 6 and the Rosenbrock schemes of order 1 and 2, (c) Hankel singular values for the BDF method of order 1, (d) the outputs of the full and the reduced-order models, and (e) relative errors in the output.

with

$$G_{k2} = \begin{bmatrix} N_{k+1}, & A_{k+1}L_k, & EL_k, & A_{k+1}R_1, & ER_1 \end{bmatrix},$$
$$S_{k2} = \begin{bmatrix} I_{\tilde{n}_{k+1}} & & & & \\ & D_k & & & \\ & & D_k & & \\ & & & M_1 & \\ & & & M_1 & -\frac{2}{\tau_k}M_1 \end{bmatrix}. \tag{16}$$

Therefore, the solution K_2 of (15) can be computed in the form $K_2 \approx R_2 M_2 R_2^T$ with $R_2 \in \mathbb{R}^{n\times r_2}$ and $M_2 \in \mathbb{R}^{r_2\times r_2}$ yielding a low-rank symmetric indefinite factorization $X_{k+1} \approx L_{k+1} D_{k+1} L_{k+1}^T$ with

$$L_{k+1} = \begin{bmatrix} L_k, & R_1, & R_2 \end{bmatrix}, \qquad D_{k+1} = \begin{bmatrix} D_k & & \\ & \frac{3}{2}M_1 & \\ & & \frac{1}{2}M_2 \end{bmatrix}.$$

The Rosenbrock methods of higher order can be extended to the DLE (8) in a similar way.

4 Solving the reduced-order system

In this section, we present two approaches for solving the reduced-order model (2), (6) using the BDF methods.

Approach I: Approximating the derivatives of the reduced state $\hat{x}(t)$ and the projection matrix $Z(t)$ at $t = t_k$ by

$$\dot{\hat{x}}(t_k) \approx \frac{1}{\tau_k \beta} \sum_{j=0}^{s} \alpha_j \hat{x}_{k-j}, \qquad \dot{Z}(t_k) \approx \frac{1}{\tau_k \beta} \sum_{j=0}^{s} \alpha_j Z_{k-j},$$

where $\hat{x}_j$ is an approximation to $\hat{x}(t_j)$, $Z_j = Z(t_j)$ and α_j, β are given in Table 1, we obtain from (2), (6) that

$$\hat{E}_k \frac{1}{\tau_k \beta} \sum_{j=0}^{s} \alpha_j \hat{x}_{k-j} = \Big(\hat{A}_k - \frac{1}{\tau_k \beta} W_k^T E_k \sum_{j=0}^{s} \alpha_j Z_{k-j}\Big)\hat{x}_k + \hat{B}_k u_k$$

with $\hat{E}_k = \hat{E}(t_k)$, $\hat{A}_k = \hat{A}(t_k)$, $\hat{B}_k = \hat{B}(t_k)$, $W_k = W(t_k)$, and $u_k = u(t_k)$. Then the approximate solution $\hat{x}_k$ at time t_k is determined by solving the linear system

$$\Big(2\alpha_0 \hat{E}_k - \tau_k \beta \hat{A}_k + W_k^T E_k \sum_{j=1}^{s} \alpha_j Z_{k-j}\Big)\hat{x}_k = -\hat{E}_k \sum_{j=1}^{s} \alpha_j \hat{x}_{k-j} + \tau_k \beta \hat{B}_k u_k.$$

For $s = 1$, this formula simplifies to the implicit Euler method

$$\left(2\hat{E}_k - \tau_k \hat{A}_k - W_k^T E_k Z_{k-1}\right)\hat{x}_k = \hat{E}_k \hat{x}_{k-1} + \tau_k \hat{B}_k u_k. \tag{17}$$

Note that for Approach I, the dimension of the reduced-order systems needs to be equal over the entire time horizon. This directly leads to the need of a strategy to decide for a fixed reduced dimension valid for all time instances.

Approach II: An alternative approach for solving the reduced-order model (2), (6) is based on an approximation of the derivative

$$\frac{d}{dt}\big(Z(t_k)\hat{x}(t_k)\big) \approx \frac{1}{\tau_k \beta}\sum_{j=0}^{s} \alpha_j Z_{k-j}\hat{x}_{k-j}$$

instead of the single derivatives $\dot{\hat{x}}(t)$ and $\dot{Z}(t)$ separately. This allows us to vary the system dimension r of the reduced-order model at every time step. Substituting this approximation into the reduced-order model

$$W(t)^T E(t)\frac{d}{dt}\big(Z(t)\hat{x}(t)\big) = W(t)^T A(t) Z(t)\hat{x}(t) + W(t)^T B(t)u(t), \tag{18}$$

which is equivalent to (2), (6), yields the linear system

$$(\alpha_0 \hat{E}_k - \tau_k \beta \hat{A}_k)\hat{x}_k = -W_k^T E_k \sum_{j=1}^{s} \alpha_j Z_{k-j}\hat{x}_{k-j} + \tau_k \beta \hat{B}_k u_k.$$

Here, the expression $W_k^T E_k \sum_{j=1}^{s} \alpha_j Z_{k-j}\hat{x}_{k-j}$ realizes the possible change of system dimension by implicitly lifting the previous time solutions $\hat{x}_{k-j}$ with Z_{k-j} to the full-order space and then again reducing the state dimension with $W_k^T E_k$.

Again, for $s = 1$, we have the implicit Euler scheme

$$(\hat{E}_k - \tau_k \hat{A}_k)\hat{x}_k = W_k^T E_k Z_{k-1}\hat{x}_{k-1} + \tau_k \hat{B}_k u_k. \tag{19}$$

Note that the reduced-order model (18) can also be solved using the Rosenbrock method, whereas the application of this method to the reduced-order model (2), (6) is more involved. Furthermore, we have observed in various experiments that numerical results for Approach I are less accurate than for Approach II. Therefore, in the following section, the reduced-order models will be solved using Approach II only.

5 Numerical experiments

In this section, we present some numerical experiments for balanced truncation model reduction for LTV systems. The reduced-order models are determined by using the BDF methods of order 1, 2, 3, and 6 and the Rosenbrock schemes of order 1 and 2 for solving the DLEs (3) and (4) within the balanced truncation square root method presented in Algorithm 1. Then, the soltuions to the full order system (1) and the reduced-order model (18) are computed using the linear implicit Euler method (19) given in Approach II.

5.1 Example 1

Consider the 1D heat equation

$$\begin{aligned} &c\rho\frac{\partial\theta}{\partial t}(t,z) = \kappa\frac{\partial^2\theta}{\partial z^2}(t,z) + \delta(z-\xi(t))u(t), && (t,z) \in (0,T)\times(0,\ell),\\ &\theta(t,0) = 0, \quad \theta(t,\ell) = 0, && t \in (0,T),\\ &\theta(0,z) = 0, && z \in (0,\ell), \end{aligned} \tag{20}$$

with a moving heat source which describes the heat transfer along a beam of length ℓ. Here, $\theta(t,z)$ is the temperature distribution, c, ρ and κ are the specific heat capacity, the mass density and the heat conductivity, respectively. Furthermore, $\delta(z)$ denotes the Dirac delta function, and $\xi(t)$ and $u(t)$ describe, respectively, the position and the intensity of the heat source at time t. A finite element discretization of (20) with $n+2$ equidistant grid points leads to system (1) with the time-invariant state matrices $E, A \in \mathbb{R}^{n\times n}$ and the time-varying input matrix $B(t) \in \mathbb{R}^n$. Taking the output matrix as $C(t) = B(t)^T$ corresponds to the observation of the temperature at the same position as the heat source. Since, $E = E^T$, $A = A^T$, $B = C^T$, and the initial condition of the reachability DLE (3) and the final condition of the observability DLE (4) are also equal, we obtain $P(t) = Q(T-t)$ for $t \in [0,T]$. Thus, we only have to solve one DLE in Step 1 of Algorithm 1. We consider a system dimension of $n = 2500$ and the time horizon $t \in [0, 100]s$ with a time step size $\tau = 1s$. The heat source is chosen to be $u(t) = 50$ and $\xi(t) = (\ell t)/T$. In this example, the truncation tolerance for the Hankel singular values is $1e$-10.

Figure 1 shows the dimensions of the reduced-order models corresponding to solutions of the DLEs based on the different DLE solvers (a), the Hankel singular values σ_1, σ_3, and σ_6 for all integrators (b) and the decay of the Hankel singular values on the entire time horizon (c), respectively. The system outputs of the full and the reduced-order models, as well as the related relative errors are depicted in Figures 1(d) and 1(e). From these figures one observes that all considered